



## $\mathcal{R}$ : A quantitative measure of NMR signal receiving efficiency

Huaping Mo<sup>a,b,\*</sup>, John Harwood<sup>a,c</sup>, Shucha Zhang<sup>c</sup>, Yi Xue<sup>c</sup>, Robert Santini<sup>c</sup>, Daniel Raftery<sup>c</sup>

<sup>a</sup> Purdue Interdepartmental NMR Facility, Purdue University, West Lafayette, IN 47907, USA

<sup>b</sup> Department of Medicinal Chemistry and Molecular Pharmacology, Purdue University, West Lafayette, IN 47907, USA

<sup>c</sup> Department of Chemistry, Purdue University, West Lafayette, IN 47907, USA

### ARTICLE INFO

#### Article history:

Received 3 March 2009

Revised 17 June 2009

Available online 9 July 2009

#### Keywords:

NMR

Receiving efficiency

90° Pulse length

Probe tuning and matching

Concentration reference

### ABSTRACT

Recognizing that the sensitivity of NMR is influenced by factors such as conductance and dielectric constant of the sample, we propose the receiving efficiency  $\mathcal{R}$  to characterize how efficiently the NMR signal can be observed from a unit transverse magnetization in a sample under optimal probe tuning and matching conditions. Conveniently, the relative receiving efficiency can be defined as the ratio of the NMR signal induced by a unit transverse magnetization in a sample of interest and a reference solution. Based on the reciprocal relationship between excitation and observation in NMR, the relative receiving efficiency can be correlated with the 90° pulse length ( $\tau_{90}$ ). In the special case of perfect probe tuning (impedance matched to 50  $\Omega$ ),  $\mathcal{R}$  is inversely proportional to  $\tau_{90}$ . Application of the NMR receiving efficiency in quantitative analysis potentially enables a single external concentration reference for almost any sample, eliminating the need to know its exact chemical composition or detailed electromagnetic properties.

© 2009 Elsevier Inc. All rights reserved.

### 1. Introduction

Modern NMR is a robust quantitative and reproducible method with the output signal amplitude linearly proportional to the concentration for all concentration ranges. In a simple case, it has been demonstrated that such a linear relationship can be easily extended from 100 M (in the proton concentration) to less than 10  $\mu$ M [1]. The accuracy and precision of NMR have allowed determinations of site-specific <sup>13</sup>C isotope content [2]. Additionally, NMR can be a universal quantification method, because almost all organic and biological molecules and many interesting inorganic compounds readily contain protons or other nuclei observable by NMR.

However, significant challenges still exist for accurate quantitation by NMR. One of the biggest issues is that the same signal source (typically an analyte proton) may produce NMR signals of difference sizes under different conditions. Those conditions include the solution composition, excitation angle, NMR tube size, sample volume, and other geometrical or experimental parameters. Without stringent control, signal size-based quantitation can be subject to large errors.

Hence quantitation by NMR is best performed using an accurate internal concentration standard. We recently demonstrated that

protonated NMR solvents are excellent candidates for primary concentration standards, as an alternative to preparing a known reference and adding it to the solution of interest [1]. In cases of constant sample load, the ERETIC signal was suggested as an artificial reference without resorting to any physical internal concentration standard [3]. However, such approaches are limited by the assumption of a known solvent reference (or another added reference) or the ability to maintain constant sample load and probe tuning. The introduction of internal standards that may interact with analytes of interest or other sample components such as macromolecules is also a concern for a number of sample matrices.

An alternative approach is to recognize and analyze how the NMR signal amplitude is influenced by the aforementioned factors. With good laboratory practice, it is not difficult at all to control geometrical and experimental parameters so that they do not introduce errors larger than 0.5%. Thus sample load becomes the main influencing factor that is frequently beyond the operator's control. In theory, it is possible to calculate the change in sample load based on the knowledge of solution dielectric constant and conductivity. In reality, such an approach is tedious, inaccurate and not cost-effective.

Based on the principle of reciprocity, the efficiency in NMR signal detection is related to the efficiency of excitation [4–7]. Previously, quality factor (Q) and pulse length based methods have been proposed for NMR concentration determination [8,9]. Nevertheless, these methods may fail when the condition of perfect probe tuning (i.e., impedance matching to 50  $\Omega$ ) is not met, due to either

\* Corresponding author. Address: Department of Medicinal Chemistry and Molecular Pharmacology, Purdue University, 575 Stadium Mall Drive, West Lafayette, IN 47907, USA. Fax: +1 765 494 1414.

E-mail address: [hmo@purdue.edu](mailto:hmo@purdue.edu) (H. Mo).

insufficient efforts by the operator or high sample conductance. Moreover, the application of reciprocity is only an approximation as it has been realized that NMR excitation and receiving circuits actually differ slightly (Fig. 1b). (See for example, references [10,11]) In fact, it has been argued that the probe is best tuned by reception [12].

For quantitative analysis, we propose the definition of the NMR receiving efficiency  $\mathcal{R}$  to characterize how efficiently a unit magnetization can be detected by an NMR spectrometer under the best probe tuning condition. The best tuning condition refers to tuning and matching the probe for minimal RF reflection at the observe frequency in the excitation circuit (Fig. 1b). Furthermore, we argue that  $\mathcal{R}$  can be correlated to the  $90^\circ$  pulse length for a set of fixed spectrometer parameters and conditions. Hence it is possible to use a *single external concentration reference for almost any realistic sample* once this correlation is pre-calibrated.

## 2. Experimental

We used a set of samples containing 7.20 mM NaOAc and varying amount of NaCl in 1.8% D<sub>2</sub>O solution. Their preparation has been described elsewhere [1]. An additional sample containing approximately 0.3 M Na<sub>2</sub>HPO<sub>4</sub> was also prepared (Supplementary Table 1).

Sample solutions (500  $\mu$ l) were loaded into 5 mm NMR tubes (528-PP, Wilmad-Lab Glass, Buena, NJ) separately. Each sample was shimmed and the probe was tuned to the water resonance and matched for minimal reflected RF power. Receiver gain was kept constant throughout. For ease of operation, all proton pulses were centered on the water resonance. Nominal  $90^\circ$  pulse lengths were determined with constant transmitter power attenuation for all samples [18].

One dimensional proton spectra were acquired on either a Bruker Avance 800 or 500 MHz NMR spectrometer equipped with a

5 mm inverse single z-axis gradient probe operating at 25  $^\circ$ C. The proton sweep width was 10 ppm and the FID (Free induction Decay) consisted of 16 k complex data points. On the 800 MHz spectrometer, the acetate proton signal was observed after a  $90^\circ$  pulse excitation. The inter-scan delay was set to more than 60 s, which included a 4 s pre-saturation pulse (50 Hz RF field or slightly weaker). Three measurements were conducted at week 1, 2 and 7. On the 500 MHz spectrometer, three measurements were conducted within one day and the water proton was detected after a  $2.25^\circ$  pulse excitation with an inter-scan delay of 14 s. The slight difference in proton concentrations among different solutions was taken into account in receiving efficiency determination [1,16].

All FID's were exponentially line-broadened by 0.1 Hz (800 MHz) or 0.3 Hz (500 MHz), Fourier transformed, manually phased and baseline corrected. The acetate proton signal (800 MHz) was integrated over  $\pm 0.1$  ppm and the water signal (500 MHz) over  $\pm 1$  ppm from the peak center.

## 3. Theory

We use the symbol  $\mathcal{R}$  to represent the NMR receiving efficiency under fixed experimental conditions (including temperature, receiver gain and *best probe tuning*).  $\mathcal{R}$  is analogous to the extinction coefficient used in UV-Visible spectroscopy, and the sample volume  $V$  is analogous to the optical path length. If we consider all influential factors, the NMR signal amplitude (or more specifically, peak integral)  $A$  can be expressed as

$$A = A_0 * g(RG) * \mathcal{R} * c * V * \sin(\theta) * I(\theta) \quad (1)$$

In this equation,  $A_0$  is an instrument constant,  $g(RG)$  is the receiver gain function that describes the gain of FID amplitude through the receiver (which is solely dependent on the receiver gain parameter (RG) for a given spectrometer; see Fig. 1a),  $c$  is the concentration of the observed nucleus or is proportional to the concentration of the

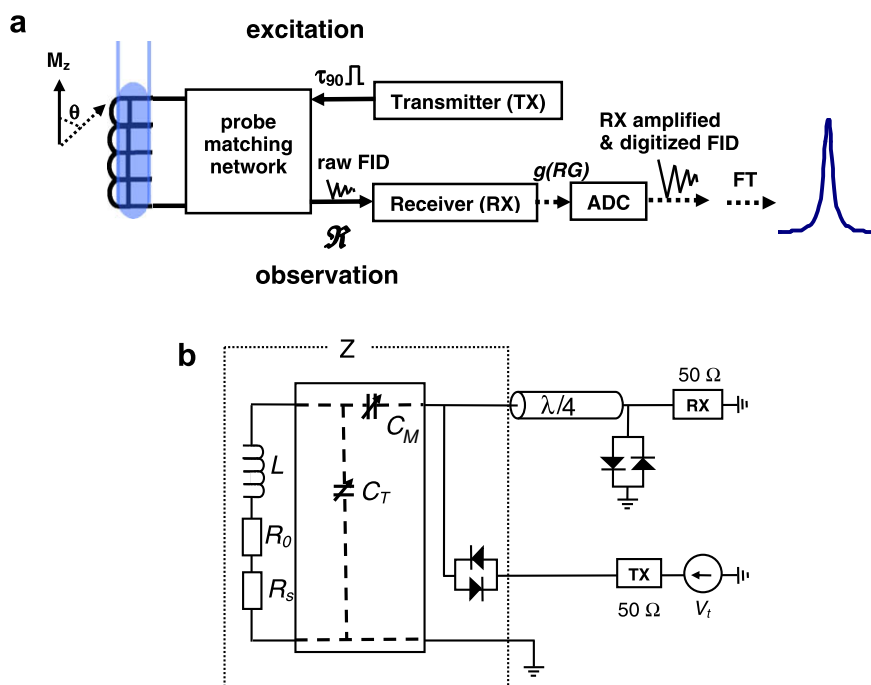


**Fig. 1.** (a) A schematic flow chart of pulse excitation and signal observation in modern high resolution NMR, and (b) the equivalent probe circuit for a typical excitation and detection. The transmitter and receiver are separated by PIN-diodes of small however finite resistance. Under the best probe tuning condition, the probe circuit impedance  $Z$  (short dashed enclosure) is tuned so that  $(Z - 50)/(Z + 50)$  approaches zero. The probe's RF coil can be represented by an inductance ( $L$ ), load-free resistance ( $R_0$ ) and sample load ( $R_s$ ). The matching network (solid enclosure) includes tunable tuning ( $C_T$ ) and matching ( $C_M$ ) capacitors. For simulations shown in Figs. 3 and 4,  $C_T$  is assumed to be parallel to  $L$  and  $C_M$  is assumed to be in a serial arrangement with respect to the transmitter/receiver.

transverse magnetization prior to detection (in case of insufficient relaxation delay and/or variable temperatures),  $\theta$  is the excitation angle, and  $I(\theta)$  is an inhomogeneity factor that describes the effect of the RF field distribution over the active sample volume  $V$ .

For simplicity, we can keep  $RG$ ,  $\theta$ , and  $V$  constant. Then the NMR signal amplitude normalized by  $\mathcal{R}$  is directly proportional to the concentration. This forms the foundation of concentration determination for any interesting sample by a single external concentration reference, regardless of the analyte solution type or salt concentration.

In practice, it is beneficial to use the relative receiving efficiency  $\mathcal{R}_r$ , which is calculated as the signal size of unit magnetization normalized by that of a reference state

$$\mathcal{R}_r = \mathcal{R}/\mathcal{R}_{\text{ref}} = \frac{A/c}{A_{\text{ref}}/c_{\text{ref}}} \quad (2)$$

Such a reference state can be represented by a sample of minimal load (resistance  $R_s$  is close to zero in Fig. 1b) and its efficiency equals to 1. Essentially, the relative receiving efficiency  $\mathcal{R}_r$  quantitatively characterizes how the NMR signal amplitude is influenced by the sample load, which is mainly contributed by the solution's dielectric constant and conductance [13,14]. Hereafter, the NMR receiving efficiency refers to the relative receiving efficiency  $\mathcal{R}_r$  unless otherwise stated.

For a modern commercial high resolution probe of single saddle coil design, pulse excitation and signal detection are reciprocal under a first order approximation. Hence a strong correlation between  $\mathcal{R}$  and the 90° pulse length ( $\tau_{90}$ ) is expected. We would further argue that such a correlation can be empirically established and is highly reproducible under the best probe tuning condition.

The best probe tuning condition is necessary because both the pulse length and NMR signal amplitude depend on the probe tuning: a poorly tuned probe tends to have longer pulse lengths and small NMR signal amplitude and thus poorer sensitivity. In theory, if the probe is tuned for minimal RF reflection, then the sample load eventually determines the values of the tuning capacitor  $C_T$  and matching capacitor  $C_M$  (all other probe circuit components are assumed to remain constant). In some probe circuits, the interactive nature between  $C_T$  and  $C_M$  may add uncertainties to their experimental determinations [15]. However, the best probe tuning condition does guarantee that the RF reflection coefficient  $(Z - 50)/(Z + 50)$  is as close to zero as possible ( $Z$  is the overall impedance of the probe circuit shown in Fig. 1b). Then the NMR receiving efficiency can be regarded as an empirical function of  $\tau_{90}$ :

$$\mathcal{R} = f(\tau_{90}) \quad (3)$$

In the special case of perfect probe tuning ( $Z = 50 \Omega$  at the resonance frequency),

$$(\mathcal{R} * \tau_{90})|_{50\Omega} \propto 1/V_t \quad (4)$$

or

$$\mathcal{R}|_{50\Omega} = (\tau_{90})_{\text{ref}}/\tau_{90} \quad (5)$$

where  $V_t$  is the total transmitter voltage during excitation (Fig. 1b).

If a sample is non-conductive, the probe can be typically tuned to  $50 \Omega$  and  $V_t$  is a constant. For a highly conductive or salty sample, the probe circuit impedance ( $Z$ ) may not be matched to  $50 \Omega$  and  $V_t$  may become  $Z$  dependent. Nevertheless, as long as  $Z$  can be maintained constant and the spectrometer has stable performance characteristics (and without probe arcing), it is safe to assume that  $V_t$  in Eq. (4) does not change. In other words, the product of the receiving efficiency and  $\tau_{90}$  is expected to be a constant at or near a certain probe impedance value.

We choose the best probe tuning condition by the excitation for several considerations. First, it conforms to general good NMR

practice and is easy to implement. Second, the sensitivity remains the same when the probe is tuned by excitation and reception, if the receiver gain is sufficient [12]. Third, the 90° degree pulse and signal amplitude can be reproduced with ease for the same sample.

We will demonstrate by experimental data and probe circuit simulations that the definition of  $\mathcal{R}$  is meaningful and feasible, and its correlation with  $\tau_{90}$  can be easily established for a given spectrometer.

#### 4. Results

Because the acetate (or solvent) concentrations and relevant data acquisition parameters remained the same,  $\mathcal{R}$  for all other samples or measurements could be simplified as the normalized signal size ratio according to Eq. (2). Complete lists of  $\mathcal{R}$  and  $\tau_{90}$  can be found in the supplementary materials. In Fig. 2,  $\mathcal{R}$  is plotted against the corresponding  $1/\tau_{90}$  for the 800 MHz (Fig. 2a) and 500 MHz (Fig. 2b) spectrometers. The solid line in each sub-plot connects one set of experimental data (black circles). Subsequent measurements conducted either 1 and 6 weeks later (for 800 MHz) or within the same day (for 500 MHz) gave  $\mathcal{R} - \tau_{90}$  data points (red squares and green diamonds) that are positioned on or very near the previously determined data (within 3% of expected  $\mathcal{R}$  according to any measured  $\tau_{90}$ ), indicating that the correlation between  $\mathcal{R}$  and  $\tau_{90}$  not only can be determined but also is highly reproducible over reasonable periods of time.

For the same sample, the values of  $\tau_{90}$  are shown to vary up to several percent (Supplementary Tables 2 & 3) among different measurements. Especially for the 800 MHz spectrometer, the  $\tau_{90}$ 's at week 7 are consistently about 3–7% longer than those at week 1. Nevertheless, the product of  $\tau_{90}$  and  $\mathcal{R}$  remains constant for any given sample in this study, suggesting the NMR signal size corrected by  $\mathcal{R}$  is a better representation of the concentration.

For quantitative analysis, we argue that the signal size should be weighted by a factor (receiving efficiency) that takes  $\tau_{90}$  into account. This approach is especially useful when analyzing samples (i.e. bio-fluids) containing varying amount of electrolytes. In the current set of examples, if the 90° pulse length (or the receiving efficiency) difference is not considered, the concentration determination for the highly conductive sample (1.6 M NaCl) using the salt free external reference would easily lead to an underestimation of the proton concentration by more than 50%.

Overall, an inverse relationship between  $\tau_{90}$  and signal size (or  $\mathcal{R}$ ) can be seen in Fig. 2: larger  $\tau_{90}$  corresponds to diminished  $\mathcal{R}$ . Under perfect probe tuning and matching conditions, such a relationship becomes strictly quantitative as Eq. (5) suggests. The dashed lines in Fig. 2 correspond to the calculated  $\mathcal{R}$  by Eq. (5) under the assumption that it can be extended to all samples (pulse lengths). As expected, when the NaCl concentration is below 200 mM, the probe can be matched to  $50 \Omega$ . The dashed lines overlap the solid ones very well. On the other hand, when the NaCl concentration is higher than 200 mM, the probe circuit cannot be tuned to  $50 \Omega$  due to the limited range of the matching capacitor. A gradual deviation for the dashed curves is observed as the salt concentration increases. It is interesting to note that the measured  $\mathcal{R}$ 's are lower than Eq. (5) suggests at 500 MHz and higher at 800 MHz. Presumably, the root cause is that the  $V_t$  term in Eq. (4) is no longer a constant when the probe cannot be matched to  $50 \Omega$ . This observation is in disagreement with the literature suggestion that Eq. (5) leads to lower concentration estimations for salty samples [9]. In our opinion, the establishment of the correlation between  $\mathcal{R}$  and  $\tau_{90}$  allows a more accurate concentration determination for a far wider range of samples (up to 1.6 M NaCl equivalent in the current study).

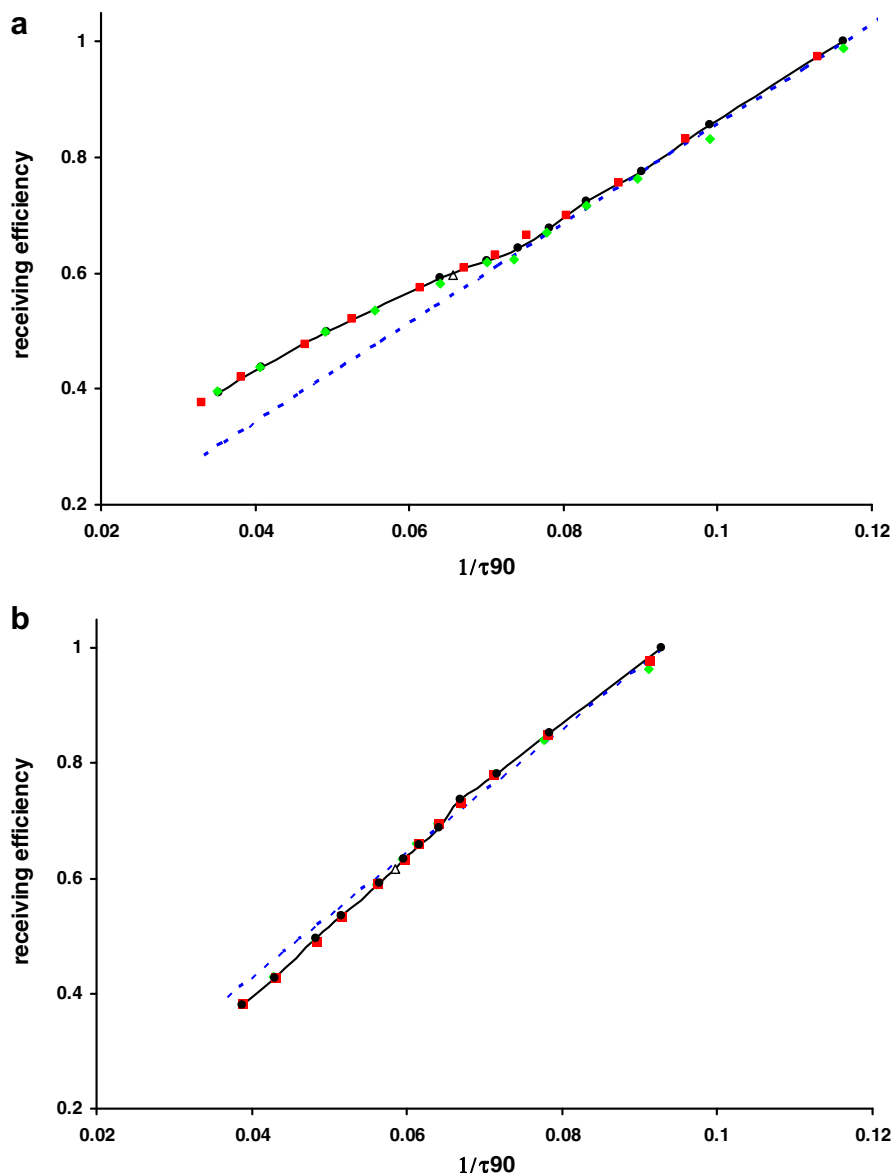


**Fig. 2.** The NMR proton receiving efficiency  $\mathcal{R}$  can be correlated to the  $90^\circ$  pulse length for an (a) 800 MHz and (b) 500 MHz NMR spectrometer. The short dashed lines are the calculated  $\mathcal{R}$  values under the assumption that Eq. (5) can be extended to long  $\tau_{90}$ 's. Experimental  $\mathcal{R}$  was determined according to Eq. (2), with sample 1 in measurement 1 used as the reference. The solid black lines simply connect the experimental data (black circles) from measurement 1 without smoothing.  $\mathcal{R}$  values are highly reproducible as repeat measurements (green diamonds and red squares) fall right on or very near to the solid lines with a maximal deviation less than 3%. Additionally,  $\mathcal{R}$  for sample 13 can be readily interpolated from the corresponding curve as 0.60 (open triangles) for (a) and 0.62 for (b), which are in excellent agreement with the expected values (Supplementary Tables 2 and 3).

The utility of such a correlation can be further demonstrated by another sample containing a different salt (about 0.3 M  $\text{Na}_2\text{H-PO}_4$ ). While the total probe resistance  $R_0 + R_s$  (Fig. 1b) can be calculated from the solution's conductivity so that  $\mathcal{R}$  can be determined by Eq. (5) [17], such a sophisticated approach is not necessary. Instead, the receiving efficiency can be interpolated as 0.60 (800 MHz) and 0.62 (500 MHz) from the corresponding  $\tau_{90}$  values (Fig. 2 triangles). Both numbers are in excellent agreement with the experimentally determined averages of 0.60 (800 MHz) and 0.62 (500 MHz) (see Supplementary Tables 2 & 3). Hence a single external concentration reference is possible for almost any realistic NMR sample, and it is not necessary to know all the details concerning solution composition or electromagnetic properties.

## 5. Discussion

For the most popular commercial NMR probe circuits, the tuning and matching capacitors are not orthogonal: slight deviation of the probe circuit impedance from  $50 \Omega$  due to under/over tuning can be largely compensated by over/under matching and vice versa [15]. As such, even for the same sample (or constant  $R_0 + R_s$  in Fig. 1b), the actual positions of the tuning and matching capacitors may not be reproduced exactly every time. The question arises as to how much error can be caused by the probe tuning uncertainty when the same sample is measured multiple times. Consequently, the correlation between  $\mathcal{R}$  and the  $90^\circ$  pulse length may become unstable in practice if  $\tau_{90}$  cannot be reliably measured. Based on practical experience, we know that  $\tau_{90}$  can be highly reproducible

for the same sample. Furthermore, we can conduct probe circuit simulations and demonstrate that uncertainties in tuning and matching do not prevent reliable measurements of  $\mathcal{R}$  and  $\tau_{90}$  either, as long as the probe is tuned and matched for minimal RF reflection.

For simplicity, we will consider a representative equivalent probe circuit shown in Fig. 1b with  $C_T$  parallel to  $L$  and  $C_M$  serial to the transmitter/receiver (other circuit types can be simulated similarly leading to the same conclusion). Typical circuit parameters are  $L = 41$  nH,  $R_0 = 0.2 \Omega$ , and the resonance frequency is 500 MHz. For a non-conductive sample,  $R_s$  can be approximated as 0. Then  $50 \Omega$  impedance matching condition requires that tuning and matching capacitance as  $C_T = 2.32$  pF and  $C_M = 0.156$  pF. In our experience, it is quite easy to achieve zero or near zero RF reflection with careful probe tuning and matching, though the mu-

tual compensative interaction between  $C_T$  and  $C_M$  may cause some uncertainties in their exact values (Fig. 3a blue region). Nevertheless, the overall impedance has to be very close to  $50 \Omega$ . As a result, the power source (transmitter) voltage  $V_T$  in Eq. (4) can be safely treated as a constant. Furthermore, the  $90^\circ$  pulse length variation (as a percentage deviation from matched condition) is well within 1% (Fig. 3b blue region). The dark blue region in Fig. 3b is much larger than that in Fig. 3a, suggesting that the  $90^\circ$  pulse length is much more tolerant to the uncertainties in  $C_T$  and  $C_M$ . Similarly, the NMR signal detected by the receiver is expected to be highly reproducible too.

In the case of a highly conductive sample, the probe circuit may not be matched to  $50 \Omega$  due to increased sample load ( $R_s$  in Fig. 1b) and the limited adjustable range of the matching capacitor. While a conductive sample can introduce additional capacitance, the equivalent probe circuit shown in Fig. 1b can still apply. For convenience, we can fix the matching capacitor to its limit before setting out to find the equivalent values for  $C_T$ ,  $C_M$ ,  $L$  and  $R_s$  at 500 MHz in Fig. 1b. First,  $L$  remains as a constant, because any realistic sample causes minimal change in magnetic permeability (or relative permeability can be treated as or very close to zero).  $R_s$  can be extrapolated from its dependence on conductivity (or NaCl concentration in the current study), the observed  $90^\circ$  pulse length, and  $R_0$ .  $C_M$  can be estimated by tuning  $C_T$  to a nearby frequency at which RF reflection is about zero (we observed 497 MHz in our set-up). Those values are very similar to those calculated for the 200 mM NaCl sample ( $R_0 = 0.2 \Omega$  and  $R_s = 0.22 \Omega$ ), as we also observed little tuning or matching capacitor position changes for samples of higher conductivity under the best tuning conditions. Hence, the initial simulation parameters for the 0.6 M NaCl solution sample on our 500 MHz spectrometer are:  $L = 41$  nH,  $R_0 = 0.2 \Omega$ ,  $R_s = 0.66 \Omega$ ,  $C_M = 0.225$  pF and  $C_T = 2.25$  pF.

The solid line in Fig. 4 is the calculated wobb RF reflection near the resonance frequency, which resembles the experimentally observed curve. The dashed line in the same figure represents the calculated  $90^\circ$  pulse length normalized by that of the load-free probe. Over a rather wide frequency range (from 499.9 to 500.1 MHz), the

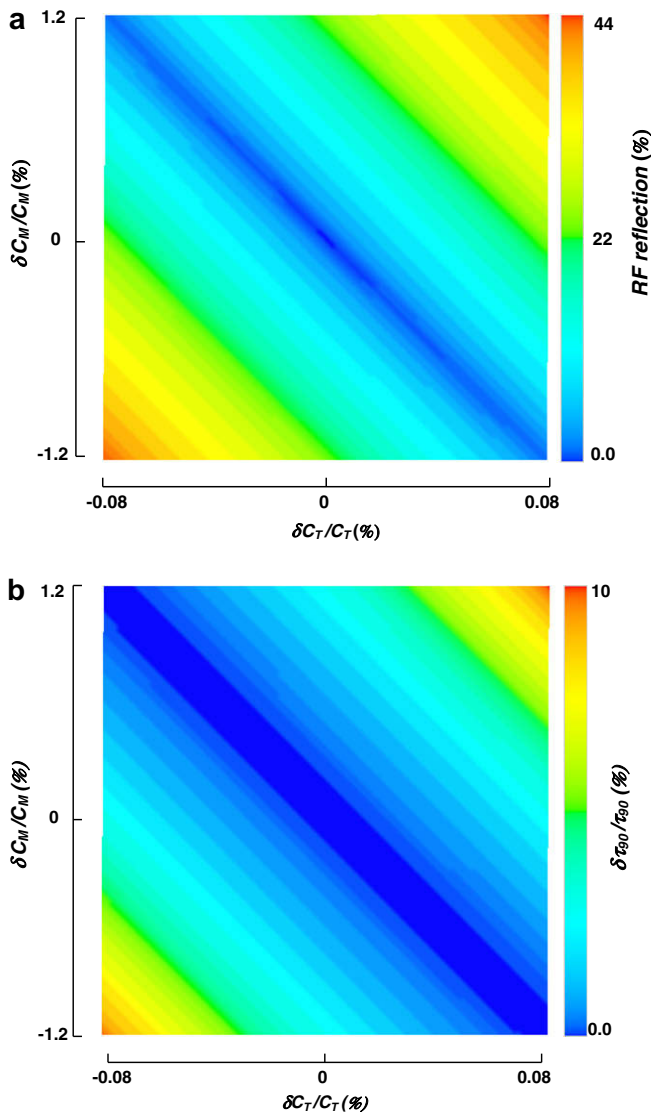


**Fig. 3.** (a) Simulated wobb RF reflection when the tuning and matching capacitors ( $C_T$  and  $C_M$ ) were perturbed near the impedance matching condition ( $50 \Omega$ ) for a typical RF circuit shown in Fig. 1b. The sample load is minimal ( $R_s = 0$ ). (b)  $90^\circ$  Pulse length deviation from the shortest value. Up to 0.8% and 1.2% changes for the optimum values are allowed for  $C_T$  and  $C_M$ . As long as RF reflection can be maintained at less than 1%, essentially the same pulse length can be obtained. Similarly, the same NMR signal amplitude can be expected. Hence, both  $\tau_{90}$  and  $\mathcal{R}$  measurements can be reproduced with ease for the same low load sample on a given spectrometer. Simulation parameters:  $C_T = 2.32$  pF,  $C_M = 0.156$  pF,  $L = 41$  nH,  $R_0 + R_s = 0.2 \Omega$ .

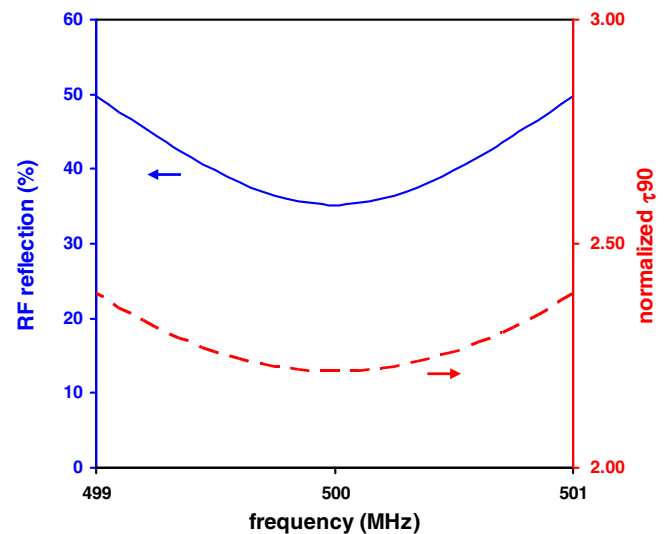


**Fig. 4.** Simulated wobb RF reflection (blue solid line) and  $90^\circ$  pulse length (red dashed line; normalized by that of the load free sample) at 500 MHz for a typical RF circuit shown in Fig. 1b with high sample load (0.6 M NaCl). The uncertainty in  $C_T$  roughly corresponds to the frequency shift for minimal RF reflection. The matching capacitor reaches its adjustable limit due to the high salt content. Between 499.9 and 500.1 MHz, both the RF reflection and  $90^\circ$  pulse length essentially remain constant (less than 1% variation). Simulation parameters:  $C_T = 2.25$  pF,  $C_M = 0.225$  pF,  $L = 41$  nH,  $R_0 + R_s = 0.86 \Omega$ .



variation among calculated  $\tau_{90}$  values is less than 1% from the median. Though the conductive sample does not allow probe impedance matching to 50  $\Omega$ , the 90° pulse length can be reproduced with ease. Based on the principle of reciprocity, the receiving efficiency can be treated as a constant near the resonance frequency as well.

The above two simulations explain why a stable pulse length and its correlation to the receiving efficiency can be readily reproduced over time. In our experience, up to 2% in  $\tau_{90}$  variation can be observed for the same sample when two independent measurements are made back-to-back. The best tuning condition, however, guarantees that the probe circuit impedance  $Z$  approaches an optimal value such that the product of relative receiving efficiency and 90° pulse length remains a constant for any realistic sample load. We have obtained plots very similar to Fig. 2 for other brands of NMR systems, including a Varian Inova 600 with an inverse probe, a Bruker Avance 500 with an inverse cryoprobe as well as another conventional inverse probe.

The concept of the NMR receiving efficiency and the determination of its dependence on  $\tau_{90}$  enable accurate quantitative analysis without introduction of any additional internal or artificial standard. Since  $\mathcal{R}$  only concerns the interaction between the transverse magnetization and the receiver, it is applicable in multidimensional NMR or when the signal is created in a non-conventional way. While the current study shows that the correlation between the 90° pulse length and the receiving efficiency can be established by a set of known standards, the latter can be calculated on the fly from a compound (such as the solvent) of a known or constant concentration for any interesting sample.

Nevertheless, it is imperative to remember that the experimentally determined receiving efficiency is not a “state function” (as used in thermodynamics) or intrinsic to a solution. Neither is it the exact NMR equivalent of extinction coefficient in UV spectroscopy. Instead,  $\mathcal{R}$  depends on both internal factors such as sample composition and external ones including the sample geometry, the probe’s electromagnetic properties, and consistent performance of the transmitter and receiver. While the extinction coefficient of an analyte is fixed for a given sample, it cannot be accurately predicted with ease in different samples. On the other hand, the receiving efficiency in NMR may not be directly transferable from one spectrometer to another, even for the same sample. Fortunately, for most applications including concentration determinations, the combination of probe and transmitter/receiver is typically fixed. Hence a pre-calibrated  $\mathcal{R}$  is possible and useful.

Other practical factors influencing the determination of  $\mathcal{R}$  include uncertainties in reproducing the best tuning and matching conditions, variation in the NMR tube size and integration errors. We measured and confirmed that the high quality NMR tubes used in this study did not contribute to more than a 0.5% active volume variation from the mean. Because of the potential variation in inner or outer tube diameters, we would argue that utilization of a co-axial insert to introduce an internal reference in the interesting sample (that is then placed in the outer tube) may lead to higher volume variations (percentage-wise). Additionally, the inner tube may have a different receiving efficiency from the outer tube, due to the RF inhomogeneity in the transverse plane [19].

Concentration determination through the use of  $\mathcal{R}$  is complementary to an internal solvent reference method that we recently developed [1]. While the solvent reference method is very tolerant to probe tuning/matching, it frequently requires the knowledge of the solvent concentration and pulse angles. In the current method, the only requirement is to reach minimal RF reflection and careful calibration of the 90° pulse length. Modern high resolution spectrometers are now capable of automatic probe tuning and pulse calibrations, and hence concentration determination can be done with greater ease.

## 6. Conclusions

We have proposed the use of the receiving efficiency  $\mathcal{R}$  to characterize how efficiently the NMR signal can be observed from a unit transverse magnetization under the best probe tuning and matching conditions. It quantitatively reflects the influence of sample load over the observed signal size. For all practical purposes, the relative receiving efficiency can be defined and obtained reproducibly from a set of known standards. We have demonstrated with experimental data and simulations that a simple correlation between  $\mathcal{R}$  and the 90° pulse length can be reliably measured for samples containing low to modestly high concentrations of electrolytes. Benefits of using the NMR receiving efficiency approach outlined here include robust and accurate determinations of compound concentration in solutions of which we have limited knowledge, based on a single external reference. The quantification error by the  $\tau_{90}$ -dependent  $\mathcal{R}$  can be limited to be about 2% or better under favorable conditions.

## Acknowledgments

The authors thank helpful discussions with Jerry Hirschinger, Ian Henry, Carl Murphy, Nagana Gowda and Narasimhamurthy Shanaiah. Partial support from the National Institutes of Health (5R01-RR-018294 and 1R01GM085291-01) is gratefully acknowledged.

## Appendix A. Supplementary data

Supplementary data associated with this article can be found, in the online version, at doi:10.1016/j.jmr.2009.07.004.

## References

- [1] H. Mo, D. Raftery, Solvent signal as an NMR concentration reference, *Anal. Chem.* 80 (2008) 9835–9839.
- [2] E. Caytan, E. Botosoa, V. Silvestre, R. Robins, S. Akoka, G. Remaud, Accurate quantitative  $^{13}\text{C}$  NMR spectroscopy: repeatability over time of site-specific  $^{13}\text{C}$  isotope ratio determination, *Anal. Chem.* 79 (2007) 8266–8269.
- [3] S. Akoka, L. Barantin, M. Trierweiler, Concentration measurement by proton NMR using the ERETIC method, *Anal. Chem.* 71 (1999) 2554–2557.
- [4] D.I. Hoult, R.E. Richards, The signal-to-noise ratio of the nuclear magnetic resonance experiment, *J. Magn. Reson.* 24 (1976) 71–85.
- [5] E.K. Insko, M.A. Elliott, J.C. Schotland, J.S. Leigh, Generalized reciprocity, *J. Magn. Reson.* 131 (1998) 111–117.
- [6] D.I. Hoult, The principle of reciprocity in signal strength calculations – a mathematical guide, *Concept Magn. Reson.* 12 (2000) 173–187.
- [7] J.J. van der Klink, The NMR reciprocity theorem for arbitrary probe geometry, *J. Magn. Reson.* 148 (2001) 147–154.
- [8] C. Gerardin, M. Haouas, C. Lorentz, F. Taulelle, NMR quantification in hydrothermal in situ syntheses, *Magn. Reson. Chem.* 38 (2000) 429–435.
- [9] G. Wider, L. Dreier, Measuring protein concentrations by NMR spectroscopy, *J. Am. Chem. Soc.* 128 (2006) 2571–2576.
- [10] D.I. Hoult, The NMR receiver: a description and analysis of design, *Prog. NMR Spect.* 12 (1978) 41–77.
- [11] J. Mispelter, M. Lupu, A. Briguet, NMR Probeheads for Biophysical and Biochemical Experiments: Theoretical Principles & Practical Guidelines, Imperial College Press, London, 2006.
- [12] D.J.-Y. Marion, H. Desvaux, An alternative tuning approach to enhance NMR signals, *J. Magn. Reson.* 193 (2008) 153–157.
- [13] D.I. Hoult, P.C. Lauterbur, The sensitivity of the zeugmatographic experiment involving human samples, *J. Magn. Reson.* 34 (1979) 425–433.
- [14] D.G. Gadian, F.N.H. Robinson, Radiofrequency losses in NMR experiments on electrically conducting samples, *J. Magn. Reson.* 34 (1979) 449–455.
- [15] F. Hwang, D.I. Hoult, Automatic probe tuning and matching, *Magn. Reson. Med.* 39 (1998) 214–222.
- [16] D.R. Lide, in: D.R. Lide (Ed.), *CRC Handbook of Chemistry and Physics*, 82nd ed., CRC Press, Boca Raton, FL, 2001 (section 8).
- [17] A.E. Kelly, H.D. Ou, R. Withers, V. Dötsch, Low-conductivity buffers for high-sensitivity NMR measurements, *J. Am. Chem. Assoc.* 124 (2002) 12013–12019.
- [18] C. Szántay, Analysis and implications of transition-band signals in high-resolution NMR, *J. Magn. Reson.* 135 (1998) 334–352.
- [19] A. Jerschow, G. Bodenhausen, Mapping the  $B_1$  field distribution with nonideal gradients in a high-resolution NMR spectrometer, *J. Magn. Reson.* 137 (1999) 108–115.